

Influence of Holocene permafrost aggradation and thaw on the paleoecology and carbon storage of a peatland complex in northwestern Canada

The Holocene
2017, Vol. 27(9) 1391–1405
© The Author(s) 2017
Reprints and permissions:
sagepub.co.uk/journalsPermissions.nav
DOI: 10.1177/0959683617693899
journals.sagepub.com/home/hol
SAGE

Nicolas Pelletier,¹ Julie Talbot,¹ David Olefeldt,^{2,3} Merritt Turetsky,²
Christian Blodau,^{4*} Oliver Sonnentag¹ and William L Quinton⁵

Abstract

Permafrost in peatlands strongly influences ecosystem characteristics, including vegetation composition, hydrological functions, and carbon cycling. Large amounts of organic carbon are stored in permafrost peatlands in northwestern Canada. Their possible degradation into permafrost-free wetlands including thermokarst bogs may affect carbon (C) stocks, but the direction and magnitude of change are uncertain. Using peat core reconstructions, we characterized the temporal and spatial variability in vegetation macrofossil, testate amoebae, C content, and peat decomposition along a permafrost thaw chronosequence in the southern portion of the Scotty Creek watershed near Fort Simpson, Northwest Territories. The accumulation of limnic and minerotrophic peat prevailed at the site until permafrost formed around 5000 cal. yr BP. Three distinct permafrost periods were identified in the permafrost peat plateau profile, while permafrost only aggraded once in the thermokarst bog profile. Permafrost thawed at ~550 and ~90 cal. yr BP in the thermokarst bog center and edge, respectively. Both allogenic (climatic shifts and wildfire) and autogenic (peat accumulation, *Sphagnum* growth) processes likely exerted control on permafrost aggradation and thaw. While apparent carbon accumulation rates (ACARs) were lower during present and past permafrost periods than during non-permafrost periods, long-term C accumulation remained similar between cores with different permafrost period lengths. Deep peat was less decomposed in the permafrost plateau compared with the thermokarst bog, which we speculate is due more to differences in peat type rather than differences in decomposition environment between these two ecosystem states. Our study highlights the importance of considering potential deep peat C losses to project the fate of thawing permafrost peat C stores.

Keywords

carbon, chronosequence, peat plateau, peatlands, permafrost, thermokarst bog

Received 28 September 2016; revised manuscript accepted 5 January 2017

Introduction

Northern peatlands store approximately 500 ± 100 Gt of carbon (C) as soil organic matter (Bridgman et al., 2006; Gorham, 1991; Yu, 2012). This C pool has become the subject of increasing attention over the last few decades because of its possible positive feedback on the climate system if large amounts of peat were to decompose in response to warmer temperatures and altered precipitation patterns (Schaefer et al., 2014; Swindles et al., 2015a; Tarnocai et al., 2009). Canadian high-latitude regions contain vast areas of permafrost, that is, perennially cryotic ground. The Canadian permafrost distribution partly overlaps with the boreal biome where most peatlands are found. Since Canadian peatlands contain more than 147 Gt of soil organic carbon and ~37% of these peatlands contain permafrost (Tarnocai and Stolbovoy, 2006), their response to permafrost thaw may have a substantial impact on future climate.

In most of the boreal region, permafrost frequently occurs as elevated, treed peat plateaus surrounded by permafrost-free peatlands (Vitt et al., 1994). The aggradation of near-surface ice in peat plateaus causes the surface to rise by 1–2 m above the unfrozen sections (Zoltai and Tarnocai, 1975), giving them distinct hydrologic characteristics and vegetation cover (Camill et al.,

2009) compared with peatlands without permafrost. Peat plateaus can cover several square kilometers but are usually much smaller (Vitt et al., 1994). Discontinuous sporadic permafrost designates areas where permafrost areal extent represents 10–50% of the landscape (Heginbottom et al., 1995). Northwestern Canada, an area dominated by a continental climate, is already affected by

¹Département de géographie, Université de Montréal, Canada

²Department of Integrative Biology, University of Guelph, Canada

³Department of Renewable Resources, University of Alberta, Canada

⁴Ecohydrology and Biogeochemistry Group, Institute of Landscape Ecology, Universität Münster, Germany

⁵Cold Regions Research Centre, Wilfrid Laurier University, Canada

*Deceased 28 July 2016

Corresponding author:

Julie Talbot, Département de géographie, Université de Montréal, Pavillon 520, chemin de la Côte-Sainte-Catherine, C. P. 6128 succursale Centre-ville, Montréal, QC H3C 3J7, Canada.
Email: j.talbot@umontreal.ca

shifts in climate related to warming. These climatic changes are expected to be most severe in northern regions, including peatland-rich boreal areas, putting peat plateaus at risk of accelerated thaw in the future (Tarnocai and Stolbovoy, 2006).

Permafrost thaw in peat plateaus has already been widely observed across the North American and Eurasian subarctic regions (Anisimov and Reneva, 2006; Baltzer et al., 2014; Camill, 2005; Cheng and Wu, 2007; Christensen et al., 2004; Helbig et al., 2016a; Lara et al., 2016; Payette et al., 2004; Sannel and Kuhry, 2011). Permafrost thaw within an ice-rich peat plateau can create thermokarst bogs or fens (Olefeldt et al., 2016). Historical patterns of thermokarst bog expansion have been linked to rising air temperature, increased fire frequency and severity, and alteration of snow cover thickness and duration (Beilman and Robinson, 2003; Camill, 2005; Christensen et al., 2004; Jones et al., 2015). Some projections suggest that the current degradation of permafrost from boreal Canada could keep accelerating over the next 100 years even if air temperature stops increasing (Koven et al., 2013; Wissler et al., 2011; Zhang et al., 2008).

Peat plateaus at the southern limit of the discontinuous permafrost zone have experienced episodes of permafrost aggradation and degradation caused by wildfire (Zoltai, 1993). However, cases of multiple cycles of permafrost aggradation and degradation at a particular location seem rare (Treat et al., 2016). Severe fire events that reduce peat thickness and alter the thermal regime of forested peat plateaus (Smith et al., 2015) can initiate or accelerate permafrost degradation, leading to subsidence and the initiation of thermokarst features (Brown et al., 2015; Myers-Smith et al., 2008; Zoltai, 1993).

Permafrost peat plateaus can accumulate C at a slower rate than the surrounding unfrozen peatland portions (Loisel et al., 2014; Robinson and Moore, 2000; Turetsky et al., 2007). Nonetheless, net ecosystem carbon balance (NECB), defined as the difference between total input and total output of C in an ecosystem, may not be different in permafrost peatlands compared with their unfrozen counterparts (Olefeldt and Roulet, 2012). The conversion of peat plateau to thermokarst bog can modify the local C exchange not only by increasing CH₄ emissions (Christensen et al., 2004; Turetsky et al., 2007; Wickland et al., 2006) but also by increasing net CO₂ sequestration (Turetsky et al., 2007; Wickland et al., 2006). These flux changes could result in an increased apparent carbon accumulation rate (ACAR) of 50–500% at the surface (Camill, 2005; Jones et al., 2013; Robinson and Moore, 2000). The increase in ACAR may be transitory but still last from centuries to millennia as suggested by chronosequence studies from Alaska (Jones et al., 2013; O'Donnell et al., 2011). While there has been much focus on the high ACAR in the surface peat of thermokarst bogs, possible deep soil organic matter loss in thawed deep peat has seldom been addressed (Jones et al., 2016; O'Donnell et al., 2012). While it was once assumed that negligible soil organic matter transformations occurred in deep peat due to anaerobic conditions, chronosequence studies suggest rapid losses of soil C post-thaw from these deeper peat layers. This deep peat anaerobic decomposition in thermokarst bogs could compensate for some of the increased plant production at the surface.

The fate of rapidly thawing permafrost is largely ignored in projections of C cycle–climate feedbacks (Schuur et al., 2015), owing to a lack of understanding on how C cycling in high-latitude ecosystems may respond to climate warming. In light of the uncertainty related to potential deep C losses in the long-term trajectory of peat C storage in permafrost peatlands, we ask the following question: how does permafrost aggradation and thaw influence C accumulation and storage in a peatland? To answer this question, we analyzed biogeochemical and paleoecological data from three peat cores located along a chronosequence from intact peat plateau to thermokarst bog in a peatland located at the southern edge of the

discontinuous permafrost zone in the Northwest Territories, Canada. Our specific objectives were to (1) identify potential drivers of permafrost aggradation and thaw, (2) characterize the spatio-temporal variability of past permafrost distribution, and (3) assess the influence of permafrost on ACAR, peat accumulation, and humification. This study provides crucial steps to assess the potential impact of climate change and accelerated permafrost thaw on C storage (including deep C storage) across the vast peatland areas of the discontinuous permafrost zone.

Study area and context

The research site is located in the southern portion of the Scotty Creek catchment (61°18'N, 121°17'W) in the lower Liard River valley, Northwest Territories, Canada (Figure 1). The mean annual temperature at Fort Simpson, 50 km to the north, is 2.8°C and annual precipitation is 387 mm, of which 48% was snow for the 1981–2010 period (Meteorological Service of Canada, 2010). The southern half of the watershed is dominated by a heterogeneous peatland landscape with discontinuous permafrost and was composed in 2009 of around 9% of lakes, 21% of channel fens, 27% of thermokarst bogs, and 43% of permafrost peat plateaus (Quinton et al., 2009). All these landscape components have a distinct hydrological function; water is shed out of the peat plateau into surrounding bogs that are in turn either hydrologically disconnected from the drainage network or connected to channel fens that ultimately drain the area (Connon et al., 2014). Characteristic water table depth in peat plateaus during summer is closely following thaw depth at 40–50 cm below surface (Helbig et al., 2016b; Quinton and Baltzer, 2013; Quinton et al., 2009), while most fens and thermokarst bogs have a mean water table depth of 15 cm between April and November (Helbig et al., 2016b).

Deglaciation took place between 11,000 and 12,000 ¹⁴C yr BP at Scotty Creek (Dyke, 2004). Following deglaciation, the site was occupied by glacial Lake McConnell. Isostatic rebound caused the drainage of most of the lake before 9000 BP revealing an important deposit of lacustrine clay and a braided delta coming from the Liard River (Smith, 1994). The accumulation of sediments and peat that followed has led to the deposition of 3–4 m of organic soils (Aylesworth and Kettles, 2000).

Permafrost in the southern Mackenzie valley, including the Scotty Creek site, is warm (near 0°C), shallow, and ice-rich (Smith et al., 2009). Areal coverage of permafrost plateaus at Scotty Creek is rapidly decreasing (Chasmer et al., 2011; Connon et al., 2014; Quinton and Baltzer, 2013; Quinton et al., 2009). This peat plateau loss is believed to be caused by air warming, heat transfer from meltwater runoff (Chasmer et al., 2011), and a positive retroactive edge effect caused by the dying of trees and the subsequent increase in solar radiation reaching the ground (Baltzer et al., 2014). Mean annual air temperature has increased by ~2°C over the last 50 years in this region, but precipitation remained stable for the same period (Quinton et al., 2009). Meanwhile, peat plateau area decreased by ~27% for the period 1947–2008 (Chasmer et al., 2011) and by 13% from 1977 to 2010 (Connon et al., 2014). The majority (72%) of the peat plateaus lost since 1947 have turned into thermokarst bogs, while the expansion of fens has been less important (Connon et al., 2014).

Peat plateaus at Scotty Creek have an open canopy of *Picea mariana* and a variable shrub cover of *Rhododendron groenlandicum* and *Vaccinium uliginosum* (Garon-Labrecque et al., 2015). Plateau ground cover is mainly composed of lichen (*Cladonia rangiferina*, *Cladonia mitis*, *Cladonia chlorophaea*) with *Sphagnum capillifolium*, *Sphagnum fuscum*, or *Pleurozium schreberi* replacing the lichen cover in some areas.

Bogs are covered by *Sphagnum* with scattered *Picea mariana* or *Larix laricina* trees <2 m in height. Other common species in

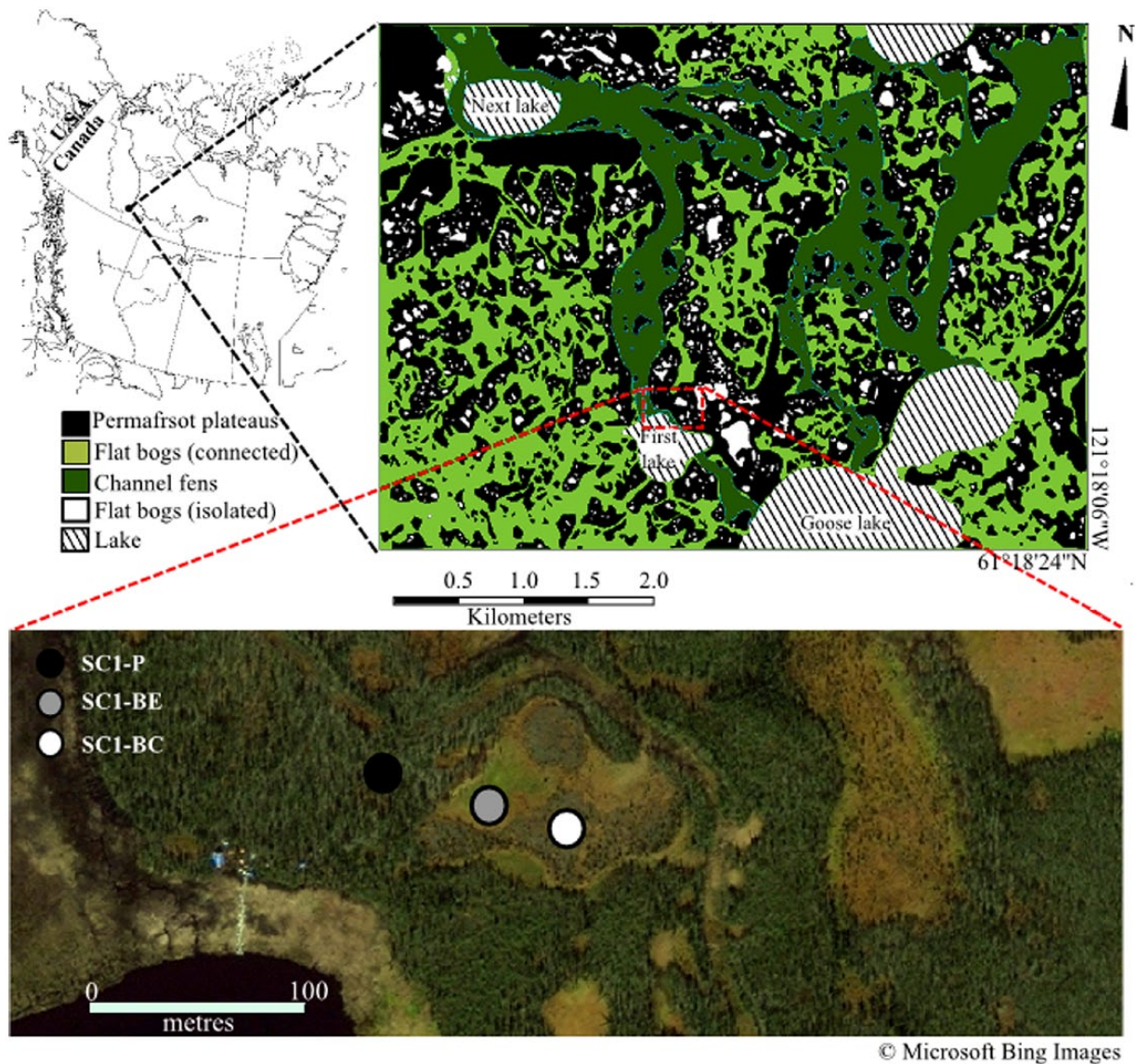


Figure 1. Site map and aerial photograph from 2015 showing coring location.

bogs include *Scheuchzeria palustris*, *Andromeda polifolia*, *Chamaedaphne calyculata*, *Vaccinium vitis-idaea*, and *Sarracenia purpurea*. *Sphagnum* species vary according to distance to thawing edges and minerotrophic sections. *Sphagnum riparium* occupies solely the most recent thaw feature (collapse scars) where standing water is visible at the surface, while *Sphagnum angustifolium* or *Sphagnum warnstorfii* dominates the sections where water table is a few centimeters below the surface. The central bog area with water table at ~10 cm is mainly covered by *Sphagnum magellanicum* and *Sphagnum fuscum*, and regrowth of young *Picea mariana* is observed in these sections.

Methods

Core collection

In July 2013, we extracted three cores along a 105-m transect extending from a peat plateau (SC1-P) to the edge of a thermokarst bog (SC1-BE) and to the center of a thermokarst bog (SC1-BC; Figure 1). Cores contain a sequence of 3.2–3.5 m of peat underlain by lacustrine silt and clay. We extracted surface cores of the upper 50 cm using 10.2-cm-diameter PVC tubes. Below 50 cm, we used a Snow, Ice, and Permafrost Research Establishment (SIPRE) coring auger (10 cm diameter) on the peat plateau and a Russian peat corer (4.5 cm diameter) on the

permafrost-free bog locations. Bog cores were taken alternating between two boreholes located ~30 cm apart, where alternating 50-cm-long sections had a 10-cm overlap. Each core section was wrapped in cellophane and placed in a PVC half-tube, frozen upon arrival to the laboratory, and then cut in 1 cm sections using a band saw.

Dating and age–depth models

Core chronologies were obtained using a combination of accelerator mass spectrometry (AMS) radiocarbon analysis, ^{210}Pb radiochronology, and identification of tephra layers. For the AMS radiocarbon dating (Table 1), 5–25 mg of clean, identifiable, and dry plant macrofossils was sent to the Carbon, Water, and Soils Laboratory at the USDA Forest Service (25 samples) and to BETA Analytic (two samples). Dates were calibrated using the IntCal13 calibration curve (Reimer et al., 2013).

The ^{210}Pb radiochronology (Supplementary Table 1, available online) was established in the thermokarst bog surficial peat by measuring the concentration of the daughter isotope ^{210}Po normally at secular equilibrium with the ^{210}Pb concentration (Flynn, 1968). Measurements were performed on an alpha spectrometer (EGG-Ortec Type 576Atm) at GEOTOP (Université du Québec, Montréal) using an acid extraction of polonium (De Vleeschouwer et al., 2010). Recent peat chronologies were calculated using

Table 1. Material used for radiocarbon dating, associated uncalibrated ages, and calibrated ages according to the Intcal13 calibration curve (Reimer et al., 2013).

Core	Depth (cm)	Sample material	Lab number	Uncalibrated age (yr BP)	1 σ calibrated age (cal. yr BP)
SCI-P	35	<i>Larix laricina</i> needles	CAMS – 170653	1875 \pm 35	1807 \pm 67
	50	<i>Polytrichum</i> spp. leaves	CAMS – 170660	2140 \pm 35	2178 \pm 118
		<i>Larix laricina</i> needles			
		<i>Picea mariana</i> needles			
	75	<i>Rhododendron groenlandicum</i> leaves	CAMS – 167869	2500 \pm 35	2608 \pm 110
	90	<i>Hamatocaulis vernicosus</i> stems and leaves	CAMS – 170661	2855 \pm 35	2956 \pm 67
	120	<i>Polytrichum</i> spp. leaves	CAMS – 171729	3680 \pm 90	3999 \pm 84
		<i>Larix laricina</i> needles			
	145	<i>Picea mariana</i> needles	CAMS – 170667	4325 \pm 35	4902 \pm 58
		<i>Drepanocladus/Hamatocaulis</i> spp. stems			
	201	<i>Hamatocaulis vernicosus</i> stems and leaves	CAMS – 167867	6140 \pm 60	7056 \pm 101
		<i>Menyanthes trifoliata</i> seeds			
	290	<i>Betula</i> spp.	CAMS – 168466	7590 \pm 35	8396 \pm 18
		<i>Carex</i> spp.			
SCI-BC		<i>Drepanocladus/Hamatocaulis</i> spp.			
	315	<i>Hamatocaulis vernicosus</i>	CAMS – 168467	8130 \pm 60	9094 \pm 96
		<i>Sphagnum</i> spp.			
	326	<i>Hamatocaulis vernicosus</i>	CAMS – 167868	8930 \pm 35	10,063 \pm 122
		<i>Sphagnum</i> spp.			
	25	<i>Sphagnum magellanicum</i> stems and leaves	CAMS – 170669	215 \pm 35	151 \pm 151
	80	<i>Larix laricina</i> needles	CAMS – 168464	570 \pm 90	587 \pm 63
	100	<i>Scheuchzeria palustris</i> stems and leaves	CAMS – 168465	425 \pm 35	493 \pm 25
	129	<i>Sphagnum riparium</i> stems and leaves	Beta – 376592	520 \pm 35	532 \pm 19
	160 ^a	Wood fragments	CAMS – 171727	7930 \pm 40	8798 \pm 155
	251	Wood fragments	CAMS – 170658	7895 \pm 40	8685 \pm 77
	317	<i>Picea mariana</i> needles	CAMS – 168296	8600 \pm 40	9554 \pm 26
		<i>Vaccinium</i> spp. leaves			
		<i>Menyanthes trifoliata</i> seeds			
SCI-BE		<i>Scorpidium</i> spp. stems and leaves			
	58	<i>Sphagnum</i> spp. stems and leaves	Beta – 376593	Modern	
	60	<i>Sphagnum</i> spp. stems and leaves	CAMS – 168470	Modern	
	73	<i>Picea mariana</i> needles	CAMS – 170663	1115 \pm 35	1016 \pm 41
		Wood fragments			
	118	<i>Aulacomnium</i> spp. stems and leaves	CAMS – 170665	2375 \pm 35	2393 \pm 46
		<i>Carex</i> spp. seeds			
		<i>Vaccinium</i> spp. leaves			
		<i>Menyanthes trifoliata</i> seeds			
	148	Sedges stems	CAMS – 171728	3455 \pm 30	3733 \pm 88
	150	<i>Rhododendron groenlandicum</i> branch and leaves	CAMS – 170659	3325 \pm 35	3545 \pm 62
	150	<i>Vaccinium vitis-idaea</i> leaves	CAMS – 170641	3600 \pm 35	3913 \pm 53
		Unidentified feather moss stems and leaves			
	200	<i>Myrica gale</i> leaves and branch	CAMS – 170650	5635 \pm 40	6410 \pm 61
	200	<i>Scorpidium</i> spp. branch and leaves	CAMS – 170662	6165 \pm 40	7082 \pm 75
		<i>Betula</i> spp. leaves			
	327	<i>Picea mariana</i> needles	CAMS – 168471	7395 \pm 35	8240 \pm 64
		<i>Rhododendron</i> spp. leaves			
		<i>Menyanthes trifoliata</i> seeds			

^aExcluded from the age–depth model because of discontinuity with other dates.

the constant-rate-of-supply model (Appleby and Oldfield, 1978), identified as the most suitable model for peatlands (Turetsky et al., 2004). Supported Pb concentrations were considered equal to the amount of ²¹⁰Pb in the deepest part of the cores where concentrations stop decreasing with depth. The eastern lobe of the White River Ash tephra layer, dated to ca. 1250 yr BP (Lerbekmo, 2008), was visually identified in all cores.

The age–depth relationship for each core was established using the *Bacon* software (Blaauw and Christen, 2011) implemented in the R computing environment (R Development Core Team, 2015). Age–depth models were estimated using a Bayesian approach where the core is divided into vertical sections. Using

over 1 million Markov Chain Monte Carlo iterations, accumulation rates were estimated for each of these sections, forming the age–depth model. We report ages as the mean of each set of iterations for a 1-cm increment with, when necessary, the minimum and maximum of the 1 σ probability distribution in brackets ([]).

Macrofossils

We described plant macrofossils every 5 cm in SC1-P and SC1-BC cores using the Mauquoy et al. (2010) protocol for preparation and identification (Supplementary Table 2, available online). For each sample, we collected 3–10 cm³ of peat from a single 1

cm depth section. We visually estimated main peat components such as *Sphagnum*, brown mosses, sedges, ligneous organic matter, lichen, and ericaceous rootlets, as percentage of peat volume using the mean of five different estimates. Five classes ($\leq 1\%$, 1–10%, >10–50%, >50–90%, and >90%) were used to estimate main peat components. Leaves, needles, and seeds were counted and reported as individuals per cubic centimeter. Ericaceous rootlets were identified by their distinct red tint in the peat that was less decomposed but were indistinguishable from other ligneous rootlets in more decomposed peat. Only above-ground sedge results were used for all vegetation reconstruction.

To identify the main transitions between macrofossil assemblages in each core, a stratigraphically constrained cluster analysis using only the above-ground macrofossils information was carried with CONISS (Grimm, 1987) implemented in the R computing environment (R Development Core Team, 2015). The *rioja* package (Juggins, 2015) was used to build the cluster tree and the *R stats* package was used to cut the tree at the desired number of clusters. Here, ‘zone’ denotes contiguous depth intervals, with macrofossils representing a similar environment. The broken-stick method was used to determine the maximum number of reliably recognizable zones (Bennett, 1996). The number of zones is considered reliable when the total variance from all zones, expressed as sum of squares, exceeds the variance predicted by a broken-stick distribution.

We assessed summary macrofossil information only for the SC1-BE core to understand peatland development at this location. Zones in SC1-BE were identified using the proportion of main peat components (brown mosses, sedges, ligneous organic matter, lichen, and ericaceous rootlets).

Testate amoebae

Testate amoebae are a polyphyletic group of microorganisms that are sensitive to humidity conditions and produce distinguishable decay-resistant tests (shells). They have recently been used as an indicator of permafrost presence in northern peatlands (Lamarre et al., 2012; Swindles et al., 2015b). We identified and counted fossil tests of testate amoebae every 10 cm in the SC1-P and SC1-BC cores (Supplementary Table 3, available online). We prepared samples for identification on microscope slides following Booth et al. (2010). Samples with very low concentrations (<10 tests per slide) were excluded from the results as it was impossible to reach a statistically significant count (150 tests) in a reasonable amount of time. We used a weighted average transfer function dataset (Lamarre et al., 2012) to estimate past water table depth variations.

Fire events

Macroscopic charcoals were prepared by submerging 1 cm³ of peat from every 1-cm section of the SC1-P core in bleach for 24 h. The residues were then placed under a stereo microscope coupled to a camera and a computer running the *ImageJ* open-source image-processing program (Rasband, 1997–2015) for automated counting and to calculate the area covered by charcoals per unit volume (Supplementary Table 4, available online).

We analyzed charcoal area per volume in combination with the age–depth models using the *CharAnalysis* program (Higuera et al., 2009) implemented in MATLAB (The MathWorks Inc., 2015) to identify the peaks in charcoal input through time, based on the assumption that char records are composed of a background component from long-distance transport and a peak component that includes noise and local fire events. Peak components (C_{peak}) were distinguished from background values (C_{back}) by applying a LOWESS smoothing (Cleveland, 1981) to the char records. C_{peak} was then further sub-divided into two population by using the 99th percentile of the C_{peak} distribution as a global

threshold: the population with the lowest mean represent long-distance charcoal (C_{noise}) input and the population with the highest mean represent local vegetation charcoal input (C_{fire}). Sections of the record that contain C_{fire} values exceeding this threshold were interpreted as local fire (Ali et al., 2009; Higuera et al., 2009; Van Bellen et al., 2012).

Fire events inferred from *CharAnalysis* can include deposition of small char particles from a nearby fire that did not necessarily burn peat or vegetation directly at the sampling location. To identify fire events that directly affected the coring location, we further sub-divided fire events (C_{fire} exceeding global threshold) into local and extra-local by calculating a size index ($C_{\text{size}} = C_{\text{area}} / C_{\text{count}}$) for the char particles using measured charcoal count (C_{count}) and charcoal area (C_{area}). We considered the top quartile of the C_{size} distribution to be the most severe and local fire events and the rest to be possible extra-local events.

Peat humification

We used C:N ratios and Fourier transform infrared (FTIR) spectroscopy characteristics to assess peat humification status every 5–10 cm. Total carbon (TC) and total nitrogen (TN) content was determined using an element analyzer Euro EA (HEKAtech GmbH, Wegberg, Germany) by burning 4–11 mg of homogenized sample. FTIR (Varian 670 IR-FT-IR Spectrometer, Palo Alto, US) spectra were used to identify characteristic functional groups after automatic background correction. A total of 2 mg of freeze-dried peat samples was pressed to a pellet with 200 mg of KBr. We recorded and averaged 32 scans with 4 cm^{−1} resolution in the range of 400–4000 cm^{−1} for each sample. Absorption bands at ~1720, ~1630, ~1510, and ~1420 cm^{−1} were, respectively, used as indicator of carbonylic and carboxylic, aromatics and aromatic or aliphatic carboxylates, aromatics, and phenolic and aliphatic structures. These moieties were considered being humic substances and reported with respect to polysaccharide moieties measured at the 1030 cm^{−1} absorption band (Niemeyer et al., 1992).

We standardized all data considering the average of all normalized ratios as a humification index (HI) because humic substances are typically enriched in carboxylic, aromatic, and phenolic compounds compared with polysaccharides (Broder et al., 2012; Holmgren and Norden, 1988). Higher HI values thus represent more humified peat.

Core carbon content

We measured bulk density (g cm^{−3}) by sub-sampling 1 cm³ of peat every 2–5 cm in each core. Permafrost plateau peat cores were sub-sampled frozen, while thermokarst bog core were sub-sampled unfrozen to reflect the field conditions in ice content and bulk density. Sub-samples were oven dried at 105°C overnight and weighted. Loss-on-ignition values were determined for each sample by burning them for 4 h at 550°C. Carbon content for each depth was determined by multiplying bulk density and TC.

We calculated ACAR for each peatland stage identified through vegetation macrofossils hierarchical clustering. The age–depth models were used to calculate the age and uncertainties. The long-term rate of carbon accumulation (LORCA) differs from ACAR in that it spans the entire core, and thus was calculated based on the total core carbon content and the peatland initiation age. Peatland initiation was considered to be the age of the first peat layer with an OM content over 80%.

Statistical analysis

We partitioned ACAR between permafrost and non-permafrost zones and used two-tailed non-paired *t* tests to determine whether differences between permafrost and non-permafrost ACAR are

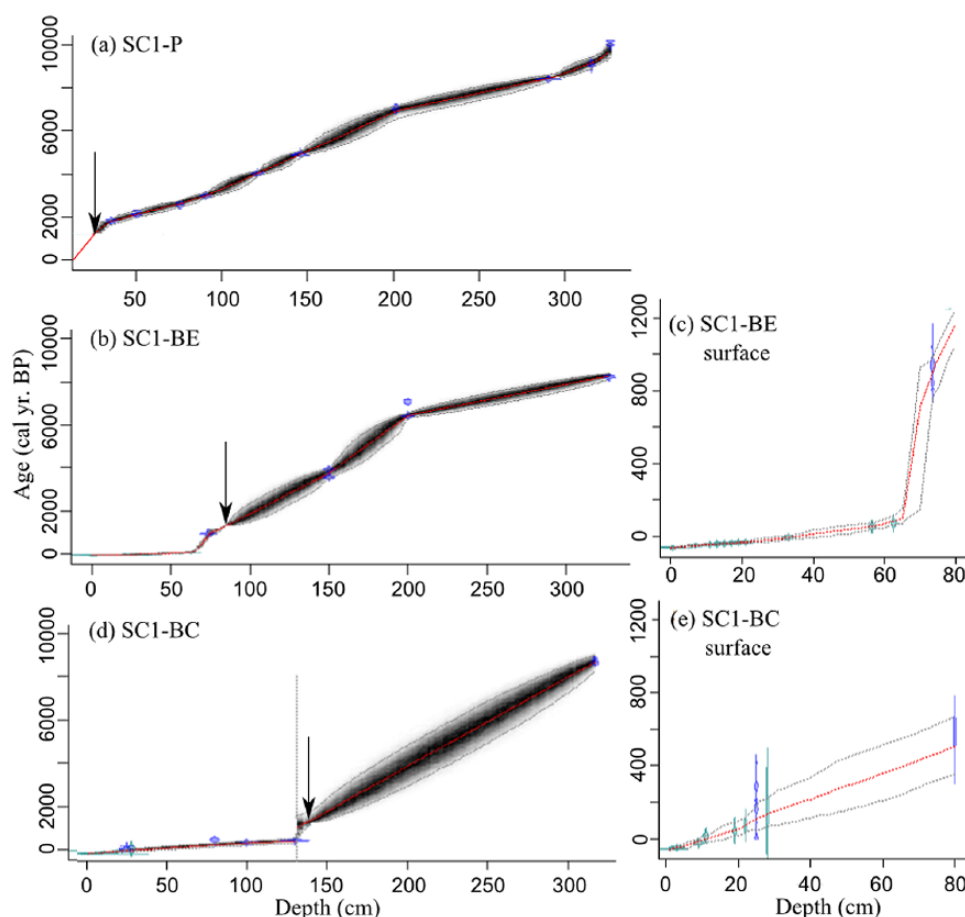


Figure 2. Bayesian age–depth models for cores (a) SC1-P, (b) SC1-BE, and (d) SC1-BC with close-ups on the surface 80 cm for cores (c) SC1-BE and (e) SC1-BC. Blue shapes represent radiocarbon calibrated age and ^{210}Pb dates. Red lines represent mean modeled ages and gray lines represent the 1σ probability distribution. Arrows indicate White River Ash tephra locations.

significant ($\alpha = 0.05$). We compared old plateau peat (>1200 years) HI and C:N ratios with old non-permafrost peat HI and C:N ratios (including fen, bog, and limnic peat) using two-tailed t tests to determine differences in humification between plateau peat and other types of peat. We also compared average deep peat HI and C:N between cores using two-tailed t tests to evaluate whether current permafrost conditions are associated with significantly different peat humification. We grouped peat layers into four types (permafrost plateau, thermokarst bog, fen, shallow water wetland) based on the zones delineated by the macrofossil analysis and their indicator taxa. We used a one-way ANOVA to determine whether peat age and peat type were significantly influencing peat humification.

Results

Age–depth models and peat accumulation rates

Basal radiocarbon ages along the transect varied between $10,063 \pm 122$ and 8240 ± 24 cal. yr BP (Figure 2). Dates inferred from ^{210}Pb chronology were within a 1σ uncertainty of radiocarbon dates where both information were available. Radiocarbon dates were generally consistent with the age–depth models, with the exception of a date inversion between 160 and 251 cm in SC1-BC (Table 1). The date from 160 cm was excluded from the database since its offset likely resulted from contamination or movement through the sediment column. Therefore, the age–depth model for the section between 134 and 251 cm in core SC1-BC has larger uncertainties. A discrepancy between the age–depth model and the radiocarbon date was also found at 129 cm in SC1-BC. A layer of char was found at this depth during

macrofossil identification (Figure 3) indicating a hiatus caused by peat burning. This hiatus was implemented in the age–depth model using the Bacon software. White River Ash tephra (1250 cal. yr BP) was found at depths of 24, 70, and 134 cm in SC1-P, SC1-BE, and SC1-BC cores, respectively.

The plateau core had less variations in vertical accumulation rates than the bog cores (Figure 2). ^{210}Pb dating revealed that accumulation rates are higher in the SC1-BE surface core than in the SC1-BC surface core. Over the last 100 years, vertical accumulation rates of both bog cores exceeded the permafrost plateau by a factor of 20 for SC1-BE and 10 for SC1-BC.

Vegetation and permafrost spatial and temporal evolution

Six and five macrofossil zones were delineated by clustering for the SC1-P core and the SC1-BC core, respectively. SC1-P clusters had to be further sub-divided as the analysis did not distinct two important transitions characterized by the alternation between humid taxa (sedges, *Menyanthes trifoliata* and/or *Scorpidium* spp.) and xeric taxa (*Picea mariana*, ericaceous rootlets, lichen). Two zones were thus added to the SC1-P core for a total of eight different zones (Table 2, Figure 4). Core SC1-BE was divided into four different zones based on summary macrofossil information (Figure 4).

Terrestrialization of a paleo-lake in the Scotty Creek basin leads to the accumulation of 50–100 cm of limnic peat starting at 8268 cal. yr BP [8106; 8382] in SC1-BE, 9688 cal. yr BP [9503; 9978] in SC1-BC, and 9310 cal. yr BP [9096; 9583] in SC1-P. Limnic peat was characterized by aquatic bryophytes taxa,

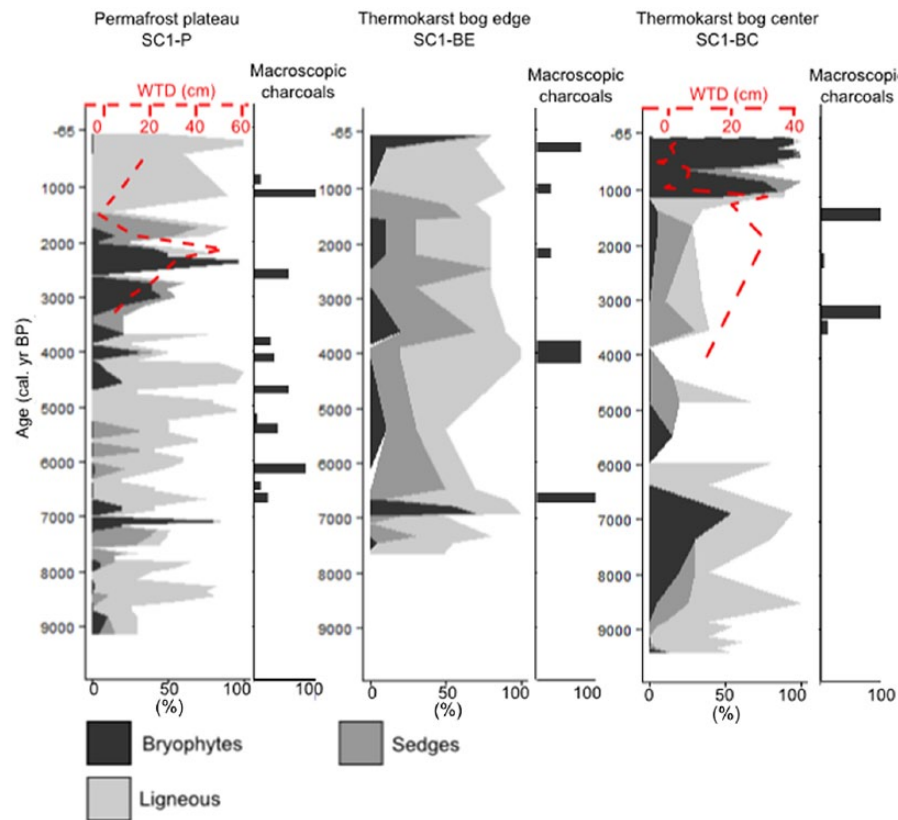


Figure 3. Main macrofossil groups and reconstructed water table depth for each core.

sedges, and various woody remains. The organic matter content in the sediments increased with continued sediment accumulation to reach ~80% at the top part of the zone.

Peatland initiation, that is, the starting point of the accumulation of sediments containing over 80% of organic matter as determined by LOI, occurred at 8890 cal. yr BP in SC1-P [8644; 9179], 7694 cal. yr BP [7348; 7921] in SC1-BE, and 8712 cal. yr BP [8238; 8905] in SC1-BC. Peat that accumulated subsequently is mainly composed of minerotrophic vegetation remains dominated by sedges, shrubs, and *Larix laricina*.

Peat that accumulated under permafrost conditions was identified based on the presence of macrofossil indicator taxa comprising *Rhododendron groenlandicum*, lichen, and large proportions of ericaceous rootlets (Table 2; Sannel and Kuhry, 2011). Three zones corresponding to peat plateau macrofossil assemblages are visible in the SC1-P core (Zone I, 25–0 cm, 1200 cal. yr BP to present; Zone II-b, 60–50 cm 2312–2114 cal. yr BP; Zone IV-a, 150–110 cm, 5063–3643 cal. yr BP) while a single zone is present in cores SC1-BE (Zone II, 83–61 cm, 1239–76 cal. yr BP) and SC1-BC (Zone III, 134–129 cm, 1215–532 cal. yr BP). In SC1-BE, a zone containing a large proportion of ligneous roots and rootlets was identified between 155 and 175 cm (5070–4050 cal. yr BP) but was not identified as permafrost peat because of the inclusion of a large amount of above-ground sedge remains in these samples. Even if some sedge species such as *Eriophorum* spp. can grow on peat plateaus, we decided to remain cautious in our delineation of permafrost periods and assumed that it would be unrealistic to think that ~30% of the peat would be composed by such species. However, this situation highlights the critical shortage of indicators of past permafrost presence in sediments.

The most recent permafrost aggradation leading the final peat plateau stage occurred synchronously in all cores at ~1235 cal. yr BP. This transition is also almost concurrent with the White River Ash deposition. Permafrost thaw subsequently occurred at 532 ± 19 cal. yr BP (129 cm) in core SC1-BC and at 76 cal. yr BP (61 cm) in core SC1-BE.

Ombrotrophic vegetation assemblages, characterized by an accumulation of *Sphagnum* and Ericaceae genera, can only be found at the surface of the SC1-BE and SC1-BC cores and in small amounts near the base of SC1-P core (Table 2, Figure 3). Given the small thickness (<10 cm) of the peat layers containing ombrotrophic taxa in the early development of SC1-P, it was not considered as ombrotrophic peat in our analysis.

Recorded permafrost thaw events were always followed by an accumulation of peat containing minerotrophic vegetation assemblages (sedges and shrubs dominance) except for the last event that lead to the current thermokarst bog phase (*Sphagnum* dominance with presence of ericaceous species).

Testate amoebae were abundant and well preserved in thermokarst bog peat but scarce or absent in permafrost plateau peat and minerotrophic peat. Low concentration of tests is common in highly humified peat and fen peat (Jauhiainen, 2002) and might be due to a low abundance of testate amoebae at deposition, the decomposition of tests, or a high abundance of material in the same size range as the tests left during preparation, rendering test detection difficult (Payne and Mitchell, 2009).

Testate amoebae assemblages indicate that water table was deeper for the intervals delimited as peat plateau, thus corroborating the presence of permafrost during these periods (Table 2, Figure 3). Due to the low number of testate amoebae samples analyzed, these results should be interpreted with caution.

Fire events

Fire events occurred at least 18 times over the last 9000 years in the Scotty Creek vicinity, but we estimate that only half of these events directly affected the current peat plateau area (Figure 5). Nine events were considered as extra-local events (fire did not reach the sampling location) because they only contained small particulate charcoal.

Regional fire frequency was highest between peat initiation and 6000 cal. yr BP with over three fire events per 1 ka (Figure 5).

Table 2. Macrofossil zone delineation with description of the paleoenvironment, indicator taxa, relative abundance of the indicator taxa (RA), relative frequency of the indicator taxa (RF), indicator value of the indicator taxa (IV, Dufrene and Legendre, 1997), *p* value of the indicator taxa, average inferred water table depth (WTD) for this zone from testate amoebae transfer function, and number of samples (*n*) analyzed for testate amoebae analysis.

	Zones	Depth (cm)	Ecosystem type	Indicator taxa	RA [cm ⁻³] (%)	RF (%)	IV	<i>p</i>	Average inferred WTD (cm)	<i>n</i>
SCI-P	PI	0–25	Peat plateau	<i>Rhododendron groenlandicum</i> leaves	[0.7]	50	27	<0.05	20 ± 10	3
				Ericaceae rootlets	(35)	100	69	<0.01		
				<i>Cladonia</i> spp.	(8)	67	48	<0.01		
	PII-a	25–50	Fen	<i>Betula cf. glandulosa</i>	[3.8]	75	23	<0.01	9	2
				<i>Cicuta bulbifera</i>	[2.3]	50	71	<0.01		
				<i>Vaccinium</i> spp. leaves	[1]	50	63	<0.01		
				<i>Rhododendron groenlandicum</i> leaves	[0.2]	50	11	<0.05		
				Sedges	(33)	75	45	<0.01		
	PII-b	50–60	Peat plateau	<i>Rhododendron groenlandicum</i> leaves	[1.2]	67	30	<0.05	32	2
				<i>Polytrichum</i> spp.	(<5)	100	60	<0.05		
				<i>Sphagnum</i> spp.	(32)	67	46	<0.05		
				Ericaceae rootlets	(7)	33	12	<0.01		
				<i>Cladonia</i> spp.	(5)	100	33	<0.01		
	PIII	60–110	Fen	<i>Larix laricina</i>	[88]	83	68	<0.01	14 ± 5	3
				<i>Menyanthes trifoliata</i> seeds	[0.6]	50	50	<0.01		
				Sedges	(10)	83	33	<0.01		
	PIV-a	110–150	Peat plateau	<i>Rhododendron groenlandicum</i> leaves	[1.9]	56	59	<0.05		0
				Ericaceae rootlets	(17)	67	48	<0.01		
				<i>Cladonia</i> spp.	(<5)	44	34	<0.01		
	PIV-b	150–190	Fen	Sedges	(11)	50	31	<0.01		0
				<i>Cladonia</i> spp.	(5)	25	33	<0.01		
	PV	190–210	Fen	<i>Larix laricina</i>	[70]	75	47	<0.01		0
				<i>Menyanthes trifoliata</i> seeds	[0.3]	75	36	<0.01		
				<i>Myrica gale</i> leaves	[7]	25	34	<0.05		
	PVI	210–315	Shallow water wetland	Sedges	(10)	50	43	<0.01		0
				<i>Scorpidium scorpioides</i>	(44)	33	46	<0.05		
				<i>Drepanocladus/Hamatocaulis</i>	(61)	17	41	<0.05		
SCI-BC	BI	0–75	Thermokarst bog	<i>Sphagnum</i> spp.	92	100	192	<0.005	7.5 ± 0.6	9
	BII	75–129	Fen	<i>Sphagnum</i> spp.	25	100	125	<0.005	7.5 ± 2.7	5
				<i>Paludella squarrosa</i>	20	63	83	<0.05		
				<i>Larix laricina</i>	<5	50	55	<0.05		
				Above-ground sedges	80	88	168	<0.05		
	BIII	129–134	Peat plateau	<i>Sphagnum</i>	<5	100	105	<0.005	25.8	2
				Ericaceae rootlets	25	67	92	<0.05		
				<i>Cladonia</i>	<5	25	30	<0.005		
	BIV	135–250	Fen	Above-ground sedges	15	70	85	<0.05	21.6	2
	BV	250–314	Shallow water wetland	<i>Alnus</i> spp.	<5	43	48	<0.05		0
				<i>Myrica gale</i>	<5	29	34			
				Above-ground sedges	<5	29	34			
				Cyperaceae seeds	<5	57	62			

Another peak period with a similar fire frequency is found between 2500 and 1500 cal. yr BP. For the last 1250 years, fire frequency was at its lowest value of the last 9000 years. Local and extra-local fire frequency was higher during permafrost periods than during non-permafrost periods.

ACARs

Average bulk density for all cores was 0.13 ± 0.08 g cm⁻³ and average C concentration was $46\% \pm 5\%$. ACAR in the limnic peat section of each core was high averaging 36.4 ± 7.5 g C m⁻² a⁻¹ ($n = 3$) and decreased as peat accumulated (Figure 6). ACAR was lower during permafrost stages compared with non-permafrost stages (even excluding the highly productive most recent thermokarst bog stage), with values of 12 g C m⁻² a⁻¹ and 19 g C m⁻² a⁻¹, respectively ($t = 2.97$, $df = 11.4$, $p < 0.01$). In non-permafrost stages, average ACAR was 16.5 ± 5.1 g C m⁻² a⁻¹ for fen stages ($n = 6$) and 82 ± 30 g C m⁻² a⁻¹ for thermokarst bog stages ($n = 2$) (including the freshly accumulated, undecomposed surface peat).

One permafrost stage in the plateau core had large uncertainties for ACAR because of its small thickness (10–15 cm). ACAR was probably overestimated for that short period, so it was removed from statistical analysis.

For the last 100 years, ACAR for the thermokarst bog peat was 145 g C m⁻² a⁻¹ at the edge (SC1-BE) and 54 g C m⁻² a⁻¹ at the center (SC1-BC), while ACAR for SC1-P for the same period is only 13 g C m⁻² a⁻¹. Accumulation rates in the bog center were higher just after permafrost thaw at ~ 100 g C m⁻² a⁻¹ and decreased to ~ 40 g C m⁻² a⁻¹ as peat accumulated. The LORCA was 20.6 g C m⁻² a⁻¹ for SC1-P, 20.1 g C m⁻² a⁻¹ for SC1-BE, and 17.7 g C m⁻² a⁻¹ for SC1-BC. The average LORCA for the entire transect was 20.6 ± 1.9 g C m⁻² a⁻¹ ($n = 3$), and the average TC concentration was 167 ± 11 kg C m⁻².

Peat humification

For all cores, the C:N ratios were higher at the top and decreased with peat depth and age (Figure 7). C:N ratios decreased more

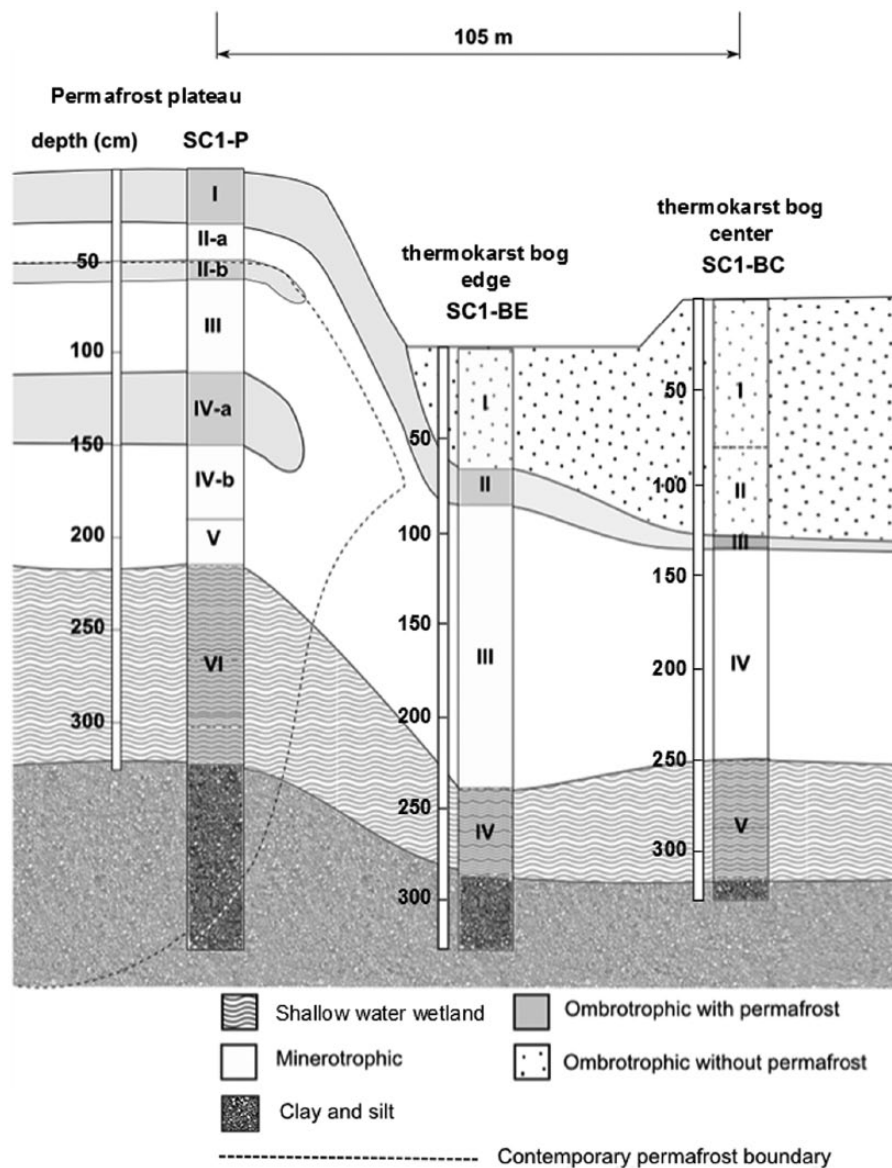


Figure 4. Schematic representation of the transect with peatland stages based on macrofossil assemblages.

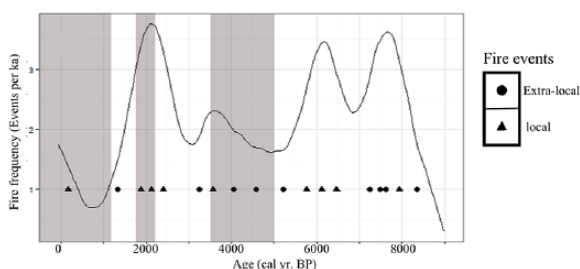


Figure 5. Gray zones represent permafrost plateau periods. Fire frequency during the last 9000 years at Scotty Creek and fire events in terms of local (affected the PLATEAU coring location) and extra-local (in the vicinity but not affecting coring location).

abruptly and stabilized at lower values in the bog central portion than at its edge or on the plateau (Figure 7). For peat buried 1 m or more below the surface (deep peat), C:N ratios varied from 20 to 45. Variance in C:N ratio was lower in the SC1-BC than in other cores. The highest C:N ratios were found near the thermokarst bog surface (~60–80 for SC1-BE and ~50 for SC1-BC).

HI was higher at the surface and tended to decrease with peat depth (Figure 7). HIs were correlated to C:N ratios ($r = 0.63$,

$p < 0.0001$) and there was a significant effect of peat age and peat type (as determined by macrofossil analysis) on HI (one-way ANOVA, $p < 0.0001$ and $p < 0.0001$, respectively) and on C:N ratio (one-way ANOVA, $p < 0.001$ and $p < 0.001$, respectively). Based on the C:N and HI, plateau peat was less humified than fen peat of similar age.

Old peat (accumulated before 1250 cal. yr BP) had a lower C:N ratio in the center of the bog compared with the plateau ($t = -2.47$, $df = 71$, $p = 0.02$) or the bog edge ($t = -1.95$, $df = 44$, $p < 0.001$). Old peat also had a higher HI in the center of the bog compared with the plateau ($t = -3.77$, $df = 72$, $p < 0.001$) or the bog edge ($p = 0.88$ for C:N and $p = 0.40$ for HI). Differences in C:N ratios or HI for old peat were not significantly different between the plateau and the bog edge ($p = 0.88$ for C:N and $p = 0.40$ for HI).

C:N ratios and HI of peat accumulated during the last 1200 years were dependent on permafrost conditions, with higher HI ($t = 4$, $df = 19$, $p < 0.001$) and lower C:N ratio ($t = -2.5$, $df = 34$, $p = 0.01$) in plateau core than thermokarst bog cores. However, for peat accumulated before 1200 cal. yr BP, the C:N ratio was higher ($t = 2.9$, $df = 16$, $p = 0.01$) and HI was lower ($t = -2.2$, $df = 18$, $p = 0.04$) for plateau peat than other types of peat. For periods where all cores had a common peat type, differences in C:N ratio or HI are not significant between cores ($p > 0.1$).

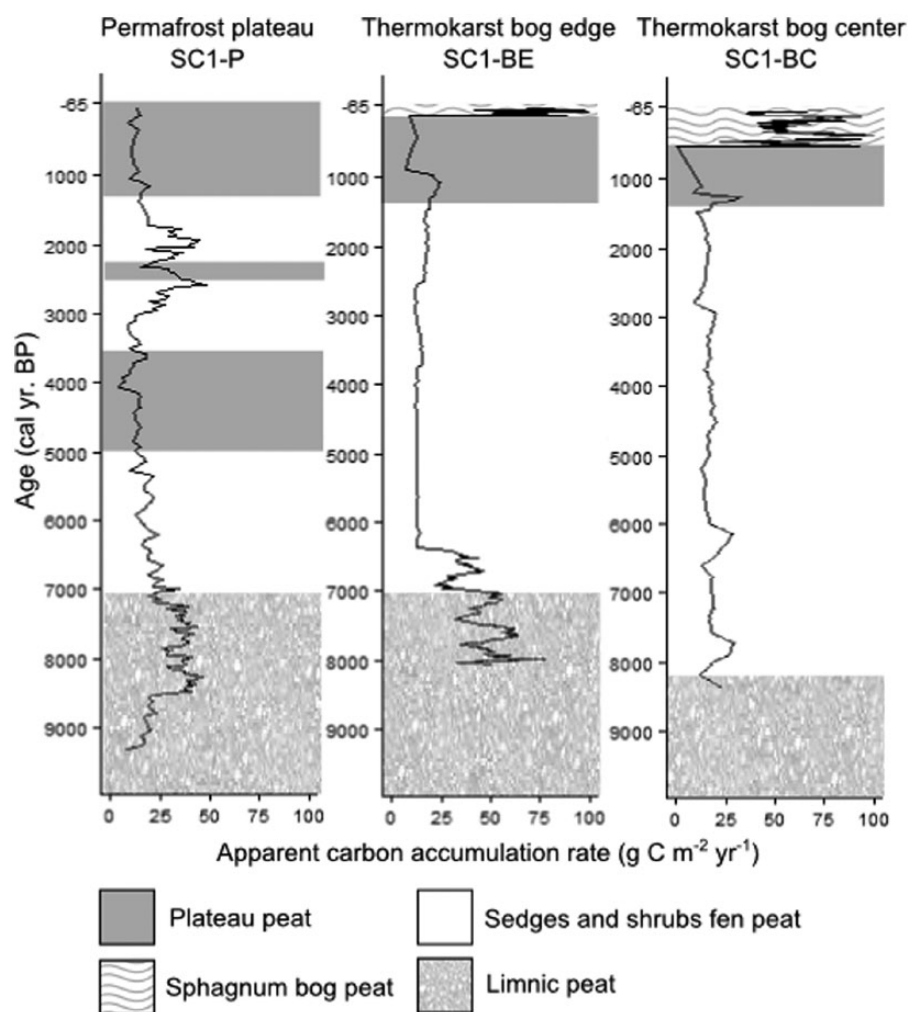


Figure 6. Apparent carbon accumulation rate for each macrofossil zone. ACAR scale is exponential. Time (in x) is the average age of each macrofossil zone.

Discussion

Permafrost aggradation and thaw at Scotty Creek

We show, in accordance with previous studies (Beilman and Robinson, 2003; Oksanen, 2006; Sannel and Kuhry, 2011; Zoltai, 1995), that the interaction of several autogenic and allogenic factors explains the timing of permafrost aggradation and thaw in peatland complexes of the discontinuous permafrost zones, such as the Scotty Creek peatland.

Climate reconstructions from the regional pollen records of central Canada suggest that temperature was slightly warmer during the period 5000–4500 cal. yr BP than during the period 6000–5000 cal. yr BP (Viau and Gajewski, 2009). The first permafrost aggradation event recorded in our chronosequence occurred at the end of the HTM at 5065 cal. yr BP. Therefore, it was unlikely to be caused by a cooling climate as air temperatures have been lower before the time of permafrost aggradation. During the 4000 years since its initiation, the peatland may have accumulated enough peat to become isolated from groundwater, with a drier surface and an insulating *Sphagnum* layer, thus modifying soil thermal properties. However, a different type of peat prior to permafrost aggradation was not detected from our macrofossil record. Dry peat has a lower thermal conductivity than wet peat and therefore loses less heat during wintertime (O'Donnell et al., 2009). A decrease in snow cover could also partly explain permafrost aggradation. A pollen reconstruction synthesis for the central Canadian region indicates that annual precipitation started to decrease around 5500 cal. yr BP (Viau and Gajewski, 2009).

Thus, the convergence of a sufficient peat accumulation and a decreasing snow cover might have been the most important drivers of permafrost aggradation at 5065 cal. yr BP. Temperatures did cool down by $\sim 1^{\circ}\text{C}$ during the period 5000–3500 cal. yr BP and precipitations slowly decreased between 5500 and 3300 cal. yr BP (Viau and Gajewski, 2009), which may explain why permafrost was stable at that time.

The period 1250–0 cal. yr BP corresponds to the coldest period since the HTM and the period with the highest precipitation (Viau and Gajewski, 2009). It is also the period where we observed permafrost aggradation in all cores. Hence, for this last permafrost event, climate cooling may have had an important role as was found for other sites located in western Canada (e.g. Beilman and Robinson, 2003; Beilman et al., 2001; Zoltai, 1993, 1995), Scandinavia (Oksanen, 2006), or northern Russia (Oksanen et al., 2001, 2003). However, this widespread permafrost aggradation event might not have happened had peat been thinner and less isolated from groundwater.

Vertical peat accumulation may also lead to a switch from minerotrophic to ombrotrophic conditions allowing colonization by *Sphagnum* mosses that rapidly accumulate soil organic matter, exacerbating the peat dryness and its insulator properties (Vardy et al., 1998; Zoltai, 1995). However, in our records, a single aggradation event of permafrost was preceded by the growth of *Sphagnum fuscum*, while the other permafrost aggradation events (5065 and 1250 cal. yr BP) were instead preceded by a dominance of sedges and shrubs, typical of a minerotrophic wetland environment. Moreover, *Sphagnum* is present in small

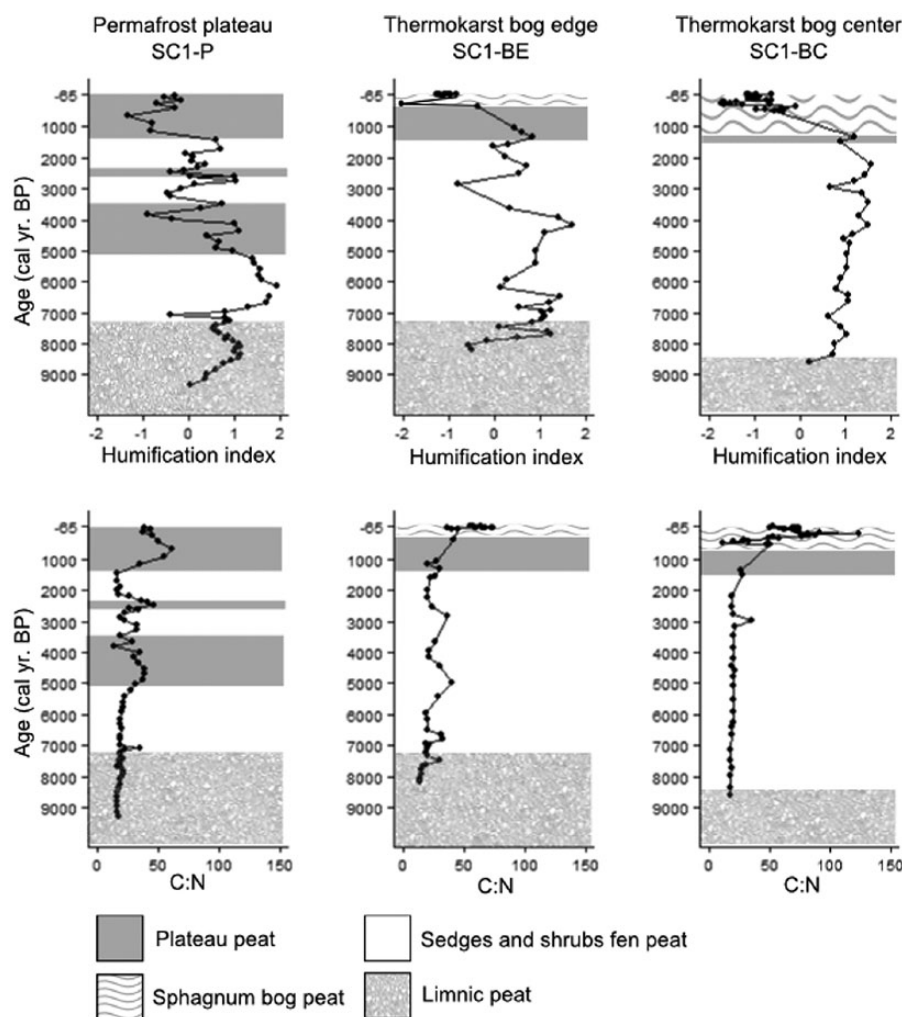


Figure 7. (a) Relationship between peat age and C:N ratio for each core; (b) relationship between peat age and peat humification index for each core.

Table 3. Pearson correlation coefficient between C:N, humification index (HI), apparent carbon accumulation rate (ACAR), number of local fire per 1 ka (fire freq.), and water table depth (WTD).

	C:N	HI	ACAR	Fire freq.
C:N				
HI	-0.63***			
ACAR	0.42***	-0.36***		
Fire freq.	-0.15	0.18	0.45***	
WTD		-0.31	-0.29	0.27

Freq: frequency.

*** $p < 0.001$.

amounts in various locations throughout the bog profiles without indications of associated permafrost aggradation. From our analysis, peat accumulation was an important driver of permafrost aggradation, but *Sphagnum* did not seem to be the main driver of this accumulation.

Climate warming (Halsey et al., 1995), increased snow cover (Johansson et al., 2013; Payette et al., 2004), and more frequent or intense fires (Zoltai, 1993) have been described as causes of permafrost thaw in boreal peatlands. We found that permafrost thaw was possibly linked to the occurrence of local fires, while there was no apparent relationship between the timing of permafrost thaw events and regional climate warming or increased precipitation rates according to the regional climate reconstruction (Viau and Gajewski, 2009). All recorded permafrost thaw

events co-occurred with local fire, but not all fire events initiated permafrost thaw. This pattern has been observed in other discontinuous permafrost peatlands where vegetation community changes following fire have been used to explain permafrost loss (e.g. Bauer and Vitt, 2011; Zoltai, 1993). Although peatland vegetation may be relatively resilient to change under typical fire conditions (Turetsky et al., 2015), more severe fire events could be important factors explaining permafrost loss, especially where permafrost is already less resilient. Fire can initiate or aggravate permafrost thaw by increasing snow cover, burning insulating peat layers, increasing the active layer depth, and favoring water ponding (Jorgenson et al., 2010; Turetsky et al., 2011; Yi et al., 2009; Zoltai, 1993).

Spatial variability in peatland development

At the Scotty Creek site, autogenic factors such as peat accumulation and vegetation changes likely allowed the aggradation of permafrost, sometimes with a contribution from a cooling climate. Allogenic factors such as climate and fire initiated permafrost thaw. Autogenic factors have likely not influenced permafrost aggradation in a spatially homogeneous way throughout peatland development, as differences exist in the permafrost history even at a relatively fine scale (tens of meters). Moreover, permafrost thaw events caused by fire are also contributing to differences in permafrost history since fires are temporally stochastic events that affect peat plateaus more severely and more frequently than thawed peatland portions (Camill et al., 2009). Fine-scale differences in peatland development history are probably common to

most boreal peatlands at the southern boundary of the discontinuous sporadic permafrost zone where permafrost is already at disequilibrium with annual air temperatures (Camill and Clark, 1998; Halsey et al., 1995). This spatial heterogeneity highlights the need to sample multiple cores from a single site when reconstructing paleoenvironmental conditions in boreal peatlands susceptible to localized permafrost aggradation.

Thermokarst bog peat type was absent from all cores before the last permafrost thaw event started. It is likely that the more widespread distribution of permafrost in this area after 1250 cal. yr BP modified drainage patterns and created areas that were separated from local hydrology. Thus, thermokarst bogs in the Scotty Creek watershed might be a relatively recent feature that could become rarer as permafrost thaws and hydrological connectivity increases, a situation where fens may become predominant again, as seen for a thawing permafrost peatland in Sweden (Swindles et al., 2015a). An increase in bogs connectivity has been observed in the lower Liard Valley over the last 40 years (Connon et al., 2014).

Effect of permafrost on carbon accumulation and lability

Permafrost periods have lower ACAR than non-permafrost periods. The ACARs calculated for the last 100 years for the thermokarst bog are three to seven times higher than the peat plateau. Yet ACARs of recorded paleo-peat-plateau in SC1-P are not significantly different than ACARs of unfrozen periods of the same age in SC1-BE and SC1-BC. Despite the fact that permafrost was apparently present more than twice as long on the peat plateau (32% of the time vs 16% and 8%, respectively, for SC1-P, SC1-BE, and SC1-BC cores), LORCA were similar between the plateau and the bog (20.6 vs 20.1 and 17.7 g C m⁻² a⁻¹). These LORCA values are of the same range than the average value of 23 ± 2 g C m⁻² a⁻¹ found by Loisel et al. (2014) for northern peatlands. The possible reasons we consider for similar ACARs in paleo-peat-plateau and non-permafrost periods are (1) lower long-term decomposition rate of plateau peat that is more recalcitrant to decomposition, (2) differential decomposition rates between peat plateau and thermokarst bog caused by environmental factors (presence of ice, temperature) or (3) inappropriate age-depth models.

Based on C:N ratios and FTIR spectral analysis, peat was more decomposed in the bog portion that was least affected by permafrost compared with the portion that was the most frequently affected by permafrost in the past. More decomposed peat in the bog section could result from increased anaerobic decomposition caused by different environmental conditions in peat during permafrost periods. However, increased anaerobic decomposition could also result from a difference in peat lability between the thermokarst bog profile and the permafrost plateau profile. It remains challenging to separate the effect of peat type and permafrost history as peat type itself is dependent on permafrost history. If the differences in deep peat decomposition between cores was caused by permafrost history, peat accumulated during periods with common peat type among cores would have a different C:N or HI depending on the core-specific permafrost history. In the chronosequence studied here, the humification of peat of similar type and age was not different among cores with different permafrost history. This suggests that the overall higher peat humification of the central bog peat likely results from a greater proportion of more labile peat rather than increased deep peat decomposition after permafrost thaw.

Peat plateaus and non-permafrost stages likely have very different C dynamics that are not apparent from the ACAR measurements, with peat plateaus slowly accumulating low-lability C and thermokarst bogs and fens rapidly accumulating high-lability C. Hence, comparing surface ACAR along a thaw chronosequence

to predict the effect of permafrost thaw on peatland C pools could generate misleading results if peat lability and long-term stability are not taken into account. Widespread permafrost degradation in boreal peatlands may lead to the rapid accumulation of C at the surface and be a negative feedback to climate change in the short term. However, if mineralization rates of peat also increase because of its high lability and the thawed of formerly frozen peat, then it is possible that this increased carbon accumulation is limited in time (Jones et al., 2016; O'Donnell et al., 2012).

Conclusion

Peatland development at Scotty Creek followed a terrestrialization succession from shallow open-water wetland to minerotrophic fen. Permafrost first aggregated at ~5000 cal. yr BP as a result of vertical peat accumulation followed by a climate cooling. Permafrost presence during the Holocene exhibits both spatial and temporal variability, which is expected for these permafrost peatlands located near the southern limit of discontinuous permafrost. Fires might have contributed to apparent cycles of aggradation and thaw in the peat sequence, but other factors are likely involved.

Thermokarst bogs are an uncommon feature in the paleoenvironment of the studied area. Minerotrophic peatlands were dominant before the first permafrost aggradation and may become dominant again if hydrological connectivity were to increase because of permafrost thaw. If this is the case, it is uncertain whether the study of a chronosequence from permafrost peat plateau to thermokarst bog can be used to predict the long-term consequences of permafrost thaw in areas where permafrost is at risk to completely disappear.

While permafrost conditions were found to reduce surface peat accumulation, our results suggest that this loss of C accumulation at the surface is compensated in the long term by the slow decomposition rate of sylvic plateau peat leading to similar LORCA between areas frequently affected by permafrost and those that were not. We postulate that the loss of boreal peat plateaus resulting from permafrost thaw will have a short-term positive effect on C accumulation that may decrease with time depending on the lability of peat accumulated during the Holocene.

Acknowledgements

Essential help with field work was provided by Masson Stothart and Andrew Kolhenberg. Chemical analyses for this paper were partly carried out in the laboratory of water air and soil analysis of ILÖK; we thank Melanie Tappe, Ulrike Metzelder, and Nicolas Kolbe for technical assistance. Thanks to Bassam Ghaleb for assistance with ²¹⁰Pb analysis and to Alayn Larouche for his contributions to peat macrofossil identification. The *CharAnalysis* program was implemented for our needs with the help of Olivier Blarquez. We also thank Zicheng Yu and two anonymous reviewers for suggestions that greatly improved the manuscript.

Funding

NP and JT were supported by funding from the Natural Sciences and Engineering Research Council of Canada (NSERC) and DO was supported by funding from the Campus Alberta Innovates Program (CAIP).

References

- Ali AA, Higuera PE, Bergeron Y et al. (2009) Comparing fire-history interpretations based on area, number and estimated volume of macroscopic charcoal in lake sediments. *Quaternary Research* 72(3): 462–468.
- Anisimov O and Reneva S (2006) Permafrost and changing climate: The Russian perspective. *AMBIO* 35(4): 169–175.

- Appleby PG and Oldfield F (1978) The calculation of lead-210 dates assuming a constant rate of supply of unsupported ^{210}Pb to the sediment. *CATENA* 5(1): 1–8.
- Aylesworth JM and Kettles IM (2000) Distribution of peatlands. In: Dyke LD and Brooks GR (eds) *The Physical Environment of the Mackenzie Valley, Northwest Territories: A Base Line for the Assessment of Environmental Change, Geological Survey of Canada Bulletin* 547: 49–55.
- Baltzer JL, Veness T, Chasmer LE et al. (2014) Forests on thawing permafrost: Fragmentation, edge effects, and net forest loss. *Global Change Biology* 20(3): 824–834.
- Bauer IE and Vitt DH (2011) Peatland dynamics in a complex landscape: Development of a fen-bog complex in the Sporadic Discontinuous Permafrost zone of northern Alberta, Canada. *Boreas* 40(4): 714–726.
- Beilman DW and Robinson SD (2003) *Peatland Permafrost Thaw and Landform Type along a Climatic Gradient* (ed Phillips M, Springman SM and Arenson LU). Leiden: Balkema Publishers, pp. 61–65.
- Beilman DW, Vitt DH and Halsey LA (2001) Localized permafrost peatlands in Western Canada: Definition, distributions, and degradation. *Arctic, Antarctic, and Alpine Research* 33(1): 70–77.
- Bennett KD (1996) Determination of the number of zones in a biostratigraphical sequence. *New Phytologist* 132(1): 155–170.
- Blaauw M and Christen JA (2011) Flexible paleoclimate age-depth models using an autoregressive gamma process. *Bayesian Analysis* 6(3): 457–474.
- Booth RK, Lamentowicz M and Charman DJ (2010) Preparation and analysis of testate amoebae in peatland paleoenvironmental studies. *Mires and Peat* 7(2): 1–7.
- Bridgman SD, Megonigal JP, Keller JK et al. (2006) The carbon balance of North American wetlands. *Wetlands* 26(4): 889–916.
- Broder T, Blodau C, Biester H et al. (2012) Peat decomposition records in three pristine ombrotrophic bogs in southern Patagonia. *Biogeosciences* 9(4): 1479–1491.
- Brown DRN, Jorgenson MT, Douglas TA et al. (2015) Interactive effects of wildfire and climate on permafrost degradation in Alaskan lowland forests. *Journal of Geophysical Research: Biogeosciences* 120(8): 1619–1637.
- Camill P (2005) Permafrost thaw accelerates in boreal peatlands during late-20th century climate warming. *Climatic Change* 68(1–2): 135–152.
- Camill P and Clark JS (1998) Climate change disequilibrium of boreal permafrost peatlands caused by local processes. *American Naturalist* 151(3): 207–222.
- Camill P, Barry A, Williams E et al. (2009) Climate-vegetation-fire interactions and their impact on long-term carbon dynamics in a boreal peatland landscape in northern Manitoba, Canada. *Journal of Geophysical Research: Biogeosciences* 114: G04017.
- Chasmer L, Quinton W, Hopkinson C et al. (2011) Vegetation canopy and radiation controls on permafrost plateau evolution within the discontinuous permafrost zone, Northwest Territories, Canada. *Permafrost and Periglacial Processes* 22(3): 199–213.
- Cheng G and Wu T (2007) Responses of permafrost to climate change and their environmental significance, Qinghai-Tibet Plateau. *Journal of Geophysical Research: Earth Surface* 112(F2): F02S03.
- Christensen TR, Johansson T, Åkerman HJ et al. (2004) Thawing sub-arctic permafrost: Effects on vegetation and methane emissions. *Geophysical Research Letters* 31(4): L04501.
- Cleveland W (1981) Lowess: A program for smoothing scatterplots by robust locally weighted regression. *American Statistician* 35(1): 54.
- Connon RF, Quinton WL, Craig JR et al. (2014) Changing hydrological connectivity due to permafrost thaw in the lower Liard River valley, NWT, Canada. *Hydrological Processes* 28(14): 4163–4178.
- De Vleeschouwer F, Sikorski J and Fagel N (2010) Development of lead-210 measurement in peat using polonium extraction: A procedural comparison. *Geochronometria* 36: 1–8.
- Dufrene M and Legendre P (1997) Species assemblages and indicator species: The need for a flexible asymmetrical approach. *Ecological Monographs* 67(3): 345–366.
- Dyke AS (2004) An outline of North American deglaciation with emphasis on central and northern Canada. *Developments in Quaternary Sciences* 2: 373–424.
- Flynn WW (1968) The determination of low levels of polonium-210 in environmental materials. *Analytica Chimica Acta* 43: 221–227.
- Garon-Labrecque MÈ, Léveillé-Bourret É, Higgins K et al. (2015) Additions to the boreal flora of the Northwest Territories with a preliminary vascular flora of Scotty Creek. *Canadian Field-Naturalist* 129(4): 349–367.
- Gorham E (1991) Northern peatlands: Role in the carbon cycle and probable responses to climatic warming. *Ecological Applications* 1: 182–195.
- Grimm EC (1987) Coniss – A Fortran-77 program for stratigraphically constrained cluster-analysis by the method of incremental sum of squares. *Computers & Geosciences* 13(1): 13–35.
- Halsey LA, Vitt DH and Zoltai SC (1995) Disequilibrium response of permafrost in boreal continental western Canada to climate change. *Climatic Change* 30(1): 57–73.
- Heginbottom JA, Dubreuil MA and Harker PA (1995) Canada – Permafrost. In: *National Atlas of Canada (MCR 4177)*. 5th edition. Ottawa: National Atlas Information Service, Natural Resources Canada, plate 2.1.
- Helbig M, Pappas C and Sonnentag O (2016a) Permafrost thaw and wildfire: Equally important drivers of boreal tree cover changes in the Taiga Plains, Canada. *Geophysical Research Letters* 43(4): 1598–1606.
- Helbig M, Wischniewski K, Kljun N et al. (2016b) Regional atmospheric cooling and wetting effect of permafrost thaw-induced boreal forest loss. *Global Change Biology* 22: 4048–4066.
- Higuera PE, Brubaker LB, Anderson PM et al. (2009) Vegetation mediated the impacts of postglacial climate change on fire regimes in the south-central Brooks Range, Alaska. *Ecological Monographs* 79(2): 201–219.
- Holmgren A and Norden B (1988) Characterization of peat samples by diffuse reflectance FT-IR spectroscopy. *Applied Spectroscopy* 42(2): 255–262.
- Jauhiainen S (2002) Testate amoebae in different types of mire following drainage and subsequent restoration. *European Journal of Protistology* 38(1): 59–72.
- Johansson M, Callaghan TV, Bosio J et al. (2013) Rapid responses of permafrost and vegetation to experimentally increased snow cover in sub-arctic Sweden. *Environmental Research Letters* 8(3): 035025.
- Jones MC, Benjamin M, Grosse G et al. (2015) Recent Arctic Tundra Fire Initiates Widespread Thermokarst Development. *Scientific Reports* 5: 15865.
- Jones MC, Booth RK, Yu Z et al. (2013) A 2200-year record of permafrost dynamics and carbon cycling in a collapse-scar bog, interior Alaska. *Ecosystems* 16(1): 1–19.
- Jones MC, Harden J, O'Donnell J et al. (2016) Rapid carbon loss and slow recovery following permafrost thaw in boreal peatlands. *Global Change Biology*. Epub ahead of print 30 June. DOI: 10.1111/gcb.13403.
- Jorgenson MT, Romanovsky V, Harden J et al. (2010) Resilience and vulnerability of permafrost to climate change. *Canadian Journal of Forest Research* 40(7): 1219–1236.

- Juggins S (2015) rioja: Analysis of quaternary science data, R package version (0.9-9). Available at: <http://cran.r-project.org/package=rioja>.
- Koven CD, Riley WJ and Stern A (2013) Analysis of permafrost thermal dynamics and response to climate change in the CMIP5 Earth System Models. *Journal of Climate* 26(6): 1877–1900.
- Lamarre A, Garneau M and Asnong H (2012) Holocene paleohydrological reconstruction and carbon accumulation of a permafrost peatland using testate amoeba and macrofossil analyses, Kuujuaupik, subarctic Québec, Canada. *Review of Palaeobotany and Palynology* 186: 131–141.
- Lara MJ, Genet H, McGuire AD et al. (2016) Thermokarst rates intensify due to climate change and forest fragmentation in an Alaskan boreal forest lowland. *Global Change Biology* 22(2): 816–829.
- Lerbekmo JF (2008) The White River Ash: Largest Holocene Plinian tephra. *Canadian Journal of Earth Sciences* 45(6): 693–700.
- Loisel J, Yu Z, Beilman D et al. (2014) A database and synthesis of northern peatland soil properties and Holocene carbon and nitrogen accumulation. *The Holocene* 24(9): 1028–1042.
- Mauquoy D, Hughes PDM and Van Geel B (2010) A protocol for plant macrofossil analysis of peat deposits. *Mires and Peat* 7(6): 1–5.
- Meteorological Service of Canada (2010) *National Climate Data Archive of Canada*. Dorval: Environment Canada.
- Myers-Smith IH, Harden JW, Wilmsking M et al. (2008) Wetland succession in a permafrost collapse: Interactions between fire and thermokarst. *Biogeosciences* 5(5): 1273–1286.
- Niemeyer J, Chen Y and Bollag J (1992) Characterization of humic acids, composts, and peat by diffuse reflectance Fourier-transform infrared-spectroscopy. *Soil Science Society of America Journal* 56(1): 135–140.
- O'Donnell JA, Harden JW, McGuire AD et al. (2011) The effect of fire and permafrost interactions on soil carbon accumulation in an upland black spruce ecosystem of interior Alaska: Implications for post-thaw carbon loss. *Global Change Biology* 17(3): 1461–1474.
- O'Donnell JA, Jorgenson MT, Harden JW et al. (2012) The effects of permafrost thaw on soil hydrologic, thermal, and carbon dynamics in an Alaskan peatland. *Ecosystems* 15(2): 213–229.
- O'Donnell JA, Romanovsky VE, Harden JW et al. (2009) The effect of moisture content on the thermal conductivity of moss and organic soil horizons from black spruce ecosystems in interior Alaska. *Soil Science* 174(12): 646–651.
- Oksanen PO (2006) Holocene development of the Vaisjeaggi palsa mire, Finnish Lapland. *Boreas* 35(1): 81–95.
- Oksanen PO, Kuhry P and Alekseeva RN (2001) Holocene development of the Rogovaya River peat plateau, European Russian Arctic. *The Holocene* 11(1): 25–40.
- Oksanen PO, Kuhry P and Alekseeva RN (2003) Holocene development and permafrost history of the Usinsk Mire, Northeast European Russia. *Géographie physique et Quaternaire* 57(2–3): 169.
- Olefelt D and Roulet NT (2012) Effects of permafrost and hydrology on the composition and transport of dissolved organic carbon (DOC) in a subarctic peatland complex. *Journal of Geophysical Research* 118: G01005.
- Olefelt D, Goswami S, Grosse G et al. (2016) Circumpolar distribution and carbon storage of thermokarst landscapes. *Nature Communications* 7: 13043.
- Payette S, Delwaide A, Caccianiga M et al. (2004) Accelerated thawing of subarctic peatland permafrost over the last 50 years. *Geophysical Research Letters* 31(18): L18208.
- Payne RJ and Mitchell EA (2009) How many is enough? Determining optimal count totals for ecological and palaeoecological studies of testate amoebae. *Journal of Paleolimnology* 42(4): 483–495.
- Quinton WL and Baltzer JL (2013) The active-layer hydrology of a peat plateau with thawing permafrost (Scotty Creek, Canada). *Hydrogeology Journal* 21(1): 201–220.
- Quinton WL, Hayashi M and Chasmer LE (2009) Peatland hydrology of discontinuous permafrost in the Northwest Territories: Overview and synthesis. *Canadian Water Resources Journal/Revue Canadienne Des Ressources Hydriques* 34(4): 311–328.
- R Development Core Team (2015) *R: A Language and Environment for Statistical Computing*. Vienna: R Foundation for Statistical Computing.
- Rasband WS (1997–2015) *ImageJ*. Bethesda, MD: U.S. National Institutes of Health. Available at: <https://imagej.nih.gov/ij/>.
- Reimer PJ, Bard E, Bayliss A et al. (2013) Intcal13 and Marine13 radiocarbon age calibration curves 0–50,000 years Cal. yr BP. *Radiocarbon* 55(4): 1869–1887.
- Robinson SD and Moore TR (2000) The influence of permafrost and fire upon carbon accumulation in high Boreal Peatlands, Northwest Territories, Canada. *Arctic, Antarctic, and Alpine Research* 32(2): 155.
- Sannel ABK and Kuhry P (2011) Warming-induced destabilization of peat plateau/thermokarst lake complexes. *Journal of Geophysical Research: Biogeosciences* 116: G03035.
- Schaefer K, Lantuit H, Romanovsky VE et al. (2014) The impact of the permafrost carbon feedback on global climate. *Environmental Research Letters* 9(8): 085003.
- Schuur EAG, McGuire AD, Schädel C et al. (2015) Climate change and the permafrost carbon feedback. *Nature* 520(7546): 171–179.
- Smith DG (1994) Glacial lake McConnell: Paleogeography, age, duration, and associated river deltas, Mackenzie river basin, western Canada. *Quaternary Science Reviews* 13(9): 829–843.
- Smith SL, Riseborough DW and Bonnaventure PP (2015) Eighteen year record of forest fire effects on ground thermal regimes and permafrost in the Central Mackenzie Valley, NWT, Canada. *Permafrost and Periglacial Processes* 26(4): 289–303.
- Smith SL, Wolfe SA, Riseborough DW et al. (2009) Active-layer characteristics and summer climatic indices, Mackenzie Valley, Northwest Territories, Canada. *Permafrost and Periglacial Processes* 20: 201–220.
- Swindles GT, Amesbury MJ, Turner TE et al. (2015b) Evaluating the use of testate amoebae for palaeohydrological reconstruction in permafrost peatlands. *Palaeogeography, Palaeoclimatology, Palaeoecology* 424: 111–122.
- Swindles GT, Morris PJ, Mullan D et al. (2015a) The long-term fate of permafrost peatlands under rapid climate warming. *Scientific Reports* 5: 17951.
- Tarnocai C and Stolbovoy V (2006) Northern peatlands: Their characteristics, development and sensitivity to climate change. Peatlands: Evolution and Records of Environmental and Climate Changes. *Developments in Earth Surface Processes* 9: 17–51.
- Tarnocai C, Canadell JG, Schuur EAG et al. (2009) Soil organic carbon pools in the northern circumpolar permafrost region. *Global Biogeochemical Cycles* 23(2): GB2023.
- The MathWorks Inc. (2015) *MATLAB and Statistics Toolbox Release*. Natick, MA: The MathWorks Inc.
- Treat CC, Jones MC, Camill P et al. (2016) Effects of permafrost aggradation on peat properties as determined from a pan-Arctic synthesis of plant macrofossils. *Journal of Geophysical Research: Biogeosciences* 121(1): 78–94.

- Turetsky MR, Benscoter B, Page S et al. (2015) Global vulnerability of peatlands to fire and carbon loss. *Nature Geoscience* 8: 11–14.
- Turetsky MR, Kane ES, Harden JW et al. (2011) Recent acceleration of biomass burning and carbon losses in Alaskan forests and peatlands. *Nature Geoscience* 4(1): 27–31.
- Turetsky MR, Manning SW and Wieder RK (2004) Dating recent peat deposits. *Wetlands* 24(2): 324–356.
- Turetsky MR, Wieder RK, Vitt DH et al. (2007) The disappearance of relict permafrost in boreal north America: Effects on peatland carbon storage and fluxes. *Global Change Biology* 13(9): 1922–1934.
- Van Bellen S, Garneau M, Ali AA et al. (2012) Did fires drive Holocene carbon sequestration in boreal ombrotrophic peatlands of eastern Canada? *Quaternary Research* 78(1): 50–59.
- Vardy SR, Warner BG and Aravena R (1998) Holocene climate and the development of a subarctic peatland near Inuvik, Northwest Territories, Canada. *Climatic Change* 40(2): 285–313.
- Viau AE and Gajewski K (2009) Reconstructing millennial-scale, regional paleoclimates of Boreal Canada during the Holocene. *Journal of Climate* 22(2): 316–330.
- Vitt DH, Halsey LA and Zoltai SC (1994) The bog landforms of Continental Western Canada in relation to climate and permafrost patterns. *Arctic and Alpine Research* 26(1): 1–13.
- Wickland KP, Striegl RG, Neff JC et al. (2006) Effects of permafrost melting on CO₂ and CH₄ exchange of a poorly drained black spruce lowland. *Journal of Geophysical Research: Biogeosciences* 111(G2): G02011.
- Wisser D, Marchenko S, Talbot J et al. (2011) Soil temperature response to 21st century global warming: The role of and some implications for peat carbon in thawing permafrost soils in North America. *Earth System Dynamics* 2(1): 161–210.
- Yi S, McGuire AD, Harden J et al. (2009) Interactions between soil thermal and hydrological dynamics in the response of Alaska ecosystems to fire disturbance. *Journal of Geophysical Research: Biogeosciences* 114(G2): G02015.
- Yu ZC (2012) Northern peatland carbon stocks and dynamics: A review. *Biogeosciences* 9(10): 4071–4085.
- Zhang Y, Chen W and Riseborough DW (2008) Transient projections of permafrost distribution in Canada during the 21st century under scenarios of climate change. *Global and Planetary Change* 60(3–4): 443–456.
- Zoltai SC (1993) Cyclic development of permafrost in the peatlands of northwestern Alberta, Canada. *Arctic and Alpine Research* 25(3): 240–246.
- Zoltai SC (1995) Permafrost distribution in peatlands of west central Canada during the Holocene warm period 6000 years B.P. *Geographie physique et Quaternaire* 49: 45–54.
- Zoltai SC and Tarnocai C (1975) Perennially frozen peatlands in the western Arctic and Subarctic of Canada. *Canadian Journal of Earth Sciences* 12: 28–43.